Thermal modelling of multilayer walls for building retrofitting applications

B. Ravelo, L. Rajaoarisoa, O. Maurice

Version of Record: https://www.sciencedirect.com/science/article/pii/S2352710219323800
Manuscript_340adfed90a182189dd50debe3f61fd1

Thermal modelling of multilayer walls for building retrofitting applications

Blaise Ravelo[a], Lala Rajaoarisoa[b,*], Olivier Maurice[c]

[a]*Nanjing University of Information Science and Technology (NUIST), School of Electronic and Information Engineering, Nanjing, Jiangsu 210044, China*
[b]*University of Lille, IMT Lille Douai, F-59000 Lille, France*
[c]*3AFSCET - Association Française de Science des Systèmes, Paris, France*

Abstract

Today the building sector consumes than third of global energy consumption. Thus, improving building envelope performance can optimize building thermal and energy efficiency. This paper introduces an original modelling of thermal dynamic in the building wall. The model will help us to understand the heat transfer mechanism of multilayer walls to better support building retrofits, in order to reduce energy consumption. The model is based on the Kron's method developed with the Tensorial Analysis of Networks (TAN). The feasibility of the model is studied with a multi-layer pieces of wall. The TAN thermal modelling methodology is described with different steps of routine algorithm. The Kron's graph equivalent model is elaborated from the Cauer thermal model applied to multi-layer structure. Then, the TAN equation traducing analytically the thermal problem is established. As results, the thermal flux through two- and five-layer of wall was determined. The effectiveness of the building wall TAN model was verified with numerical parameters from a residential building located in the north of the France, subject to a retrofit problem. The thermal loss, was estimated for different parameters of materials constituting the piece of wall, is given to perform the building retrofit strategies.

Keywords: Thermal modelling, Multilayer wall, Kron's method, Tensorial Analysis of Networks (TAN), Thermal loss, Retrofitting.

1. Introduction

To meet the environmental and ecology regulations as eco-zones, which is also recommended by the European Directive [15], the future design of buildings in the worldwide capital and big cities must challenge smart and intelligent aspects [24, 36], and especially in Europe. Behind this challenge, building must be designed by minimizing the electrical power consumption. The main parameters linked to this building performance are related to the thermal heat flow [29, 45]. The energy lost through the building walls and windows must be estimated by the architect engineers during the design phase. Therefore, the thermal performance modeling plays a major role in improving the prediction and evaluating the energy performance [4, 14, 22, 27, 35]. In this framework, the state of the art on the available literature regroups three categories of thermal model approaches which can be summarized as follows [42]:

- white box models which are based on physical knowledge of the system and thermal balance equations. These models are generally generated from energy simulation software like EnergyPlus [1], TRNSYS [5], etc;
- black box models which use only measured input/output data and statistical estimation methods (e.g. [6, 28, 30]);
- grey box models, a mix of the first two categories above. They use input/output data as well as some a priori knowledge on the system. A popular grey-box model is based on the equivalent RC networks [28, 43, 46].

The grey box model promises the possibility to indicate a minimum number of geometric and thermal parameters in function of the building specifications. Then, software 3D simulators of building structure taking into account the physical and geometrical parameters were also developed [10]. However, these models and simulators require improvements in terms of:

- Complexity: the model and design may become outstandingly complex with the building room and floor numbers, and constituting material properties [11]. In some studies, this type of input might be difficult or even impossible to recover [41].
- Computation solver: the numerical computation approach which are generally using 3D space meshing and needs a huge amount of computation time and power.

To face up this mathematical challenge, reduction methods of building thermal model were suggested [20, 31]. These techniques consist in proposing the simplest mathematical representation of the thermal structure. Rightly, based on the

*I am corresponding author
Email address: lala.rajaoarisoa@imt-lille-douai.fr (Lala Rajaoarisoa)

Nomenclature

Acronyms

TTF	thermal transfer function
LTI	linear time invariant
TAN	tensorial analysis of networks
PCB	printed circuit board

Model parameters

x	material length,	$[m]$
y	material thickness,	$[m]$
z	material width,	$[m]$
T_e	air ambient temperature,	$[^oC]$
T_{in}	input temperature,	$[^oC]$
T_{in}	input temperature,	$[^oC]$
T_{out}	output temperature,	$[^oC]$
λ_ξ	the thermal conductivity,	$[W/mK]$
ρ_ξ	the material massive density,	$[kg/m^3]$
δ_ξ	the specific heat capacity,	$[J/K]$
$R_{\xi\xi}$	thermal resistance of the branches,	$[m^2K/W]$
$C_{\xi\xi}$	thermal capacitance of the branches,	$[W/m^2K]$
$Z_{\xi\xi}$	thermal impedance of the branches,	$[\Omega]$
$\tau(\xi)$	constant time,	$[ms]$
P^m	power through the m^{th} branches,	$[W]$
P^β	thermal power flux contravariable,	$[W]$
T_β	branch temperature source,	$[^oC]$
Q^μ	mesh temperature flux covariable,	$[^oC]$
Γ_μ	mesh temperature based on TAN formalism,	$[^oC]$
Δ_T	instantaneous heat loss,	$[^oC]$

Other Symbols

β	the set of branch space
μ	the set of mesh space
ξ	wall layer number
a_i, b_i	i^{th} real coefficients for TTF-LTI
C^μ_β	connectivity matrix
G	volume loss coefficient
M_i	material number i
n, m	positive integers
n_b	the number of branches
n_m	the number of meshes
n_n	the number of nodes
s	Laplace variable

nodal [26], nonlinear constraint optimization [21], aggregation of states [13] and nonlinear thermal dynamics [23], the possibility to model multi-zones of building was emphasized. The reduced model (i.e low-order or simplified model) was successfully automatized for several cases of building [16]. Despite the modelling progress, further improvement is necessary in terms of time-dependent computational solver. With the new trends of modern smart and intelligent building designs, mathematical tools with possibility to estimate the electrical power consumption in function of the heat energy lost through the building wall are needed. In this way, we can proceed with linear thermal transfer function (TTF) model expressed as follows:

$$TTF(s) = \frac{\sum_{i=1}^{n} a_i s^i}{\sum_{i=1}^{m} b_i s^i}, \tag{1}$$

with n and m are positive integers and s is the Laplace variable. a_i and b_i are real coefficients for the TTF-linear time invariant (LTI) system.

For the fast prediction of the time-dependent dynamics of the heat flow through the modern building, low order modelling approaches have been deployed [20, 31]. But these low-order models (i.e reduced models) require further rigorous approaches to take into account the building multilayer walls [3, 18]. Thus, other techniques are proposed in the literature, for instance: a matrix method and Fourier transforms model was improved in [44] with the objective to compare the effect of each insulation layer at the inside or outside of the main wall mass. While a finite-difference model based on numerical integration of the one-dimensional (1-D) heat conduction equation was investigated in [2] and [37]. This class of models was developed in order to determine the optimum thickness of an insulation layer and the effect of differently locating on insulation layer within a multi-layered wall. This model also was developed in [8] and particularly for a multilayer walls containing phase change materials. The results of these works are promising, however the analysis is limited to using one, two, and three layers of insulation. Otherwise, this problem was mainly improved in [7] by using an electrical analogy to describe one-dimensional heat conduction and compare several walls. Let notice that in this study only the layer distribution was varied, in terms of their decrement factor and time lag. It is also the objective in [19], where a heat transfer matrix approach is used to derive a basic inequality on the effect produced by layer order on the decrement factor.

To be able to consider the multiscale parameters as the material constituting the multi-wall building (1-D, 2-D and 3-D), we propose to use an uncommon formalism based on the Ten-

sorial Analysis of Networks (TAN) for building thermal model in the present paper. This approach offers different possibilities, especially to compute different types of systems built with its electrical analogies and consider different thermal excitation. Extend the model from one and two-layer wall to a high number of layer is also possible, without any effort. So, the feasibility of TAN thermal modelling was investigated in [38, 39] for the analysis of electronic printed circuit board (PCB) structure. We would like to exploit the Cauer RC-ladder model [12, 39] to analyze the thermal dynamic of the building by means of the TAN formalism. Before the analytical investigation, we can get an overview on the brief TAN state of the art. The TAN formalism was initiated by Kron in 1930s for modelling electrical networks (reader can refer to [25] for further information). The model was efficiently explored by Maurice and his teams [32, 33, 34] in 2000s for modelling electromagnetic compatibility (EMC) of electrical and electronic complex system. The extension of the TAN formalism to perform fast and accurate calculations of multi-port PCB system was investigated into [9, 40]. With the analogy between the building structure and electrical circuit pointed out in [17], the uncommon method of TAN formalism could be an interesting candidate for the future thermal building design engineers.

To illustrate the thermal building TAN methodology, the present paper will investigate the modelling of piece multi-layer wall structure. For the better understanding, the remainder of the paper is organized in three main sections. Section 2 will formulate the problem in handling. Section 3 will present the analytical methodology of the thermal TAN modelling. The model is focused on a 2-layer and 5-layer structures as an illustrative example. An algorithm summarizing the approach will be given in section 4. The Section 5 will be dedicated to illustrate by a numerical application with a proof-of-concept structure composed of realistic physical and geometrical material parameters the effectiveness of the approach. Lastly, Section 6 will end the paper with a conclusion.

2. Problem formulation

The main problem of this study concerns the fast estimation of temperature in the building in function of the external temperature and the wall parameters. To illustrate in better way the proposed TAN thermal modelling, we consider the piece of wall as a parallelepiped slab. The geometry of the multi-layer 3D structure constituted by stacked materials M_a, M_b, M_c and M_d is shown in Fig. 1. Precisely, Fig. 1(a) illustrates the case with 2-layer wall and Fig. 1(b) for 5-layer case. Each material is supposed with length x, width z and thickness y_i, with $i = \{a, b, c, d, e\}$. The bulk of piece of wall will be defined by the geometrical sizes $x \vee 2(y_a + y_b) \wedge z$ for instance for 2-layer wall.

The lateral side of this structure is supposed surrounded by constant environment temperature T_e. The left side of the structure is heated by the t-time variant temperature $T_{in}(t) > T_e$. So, the main problem to solve can be formulated by the determination of the time dependent output temperature $T_{out}(t)$.

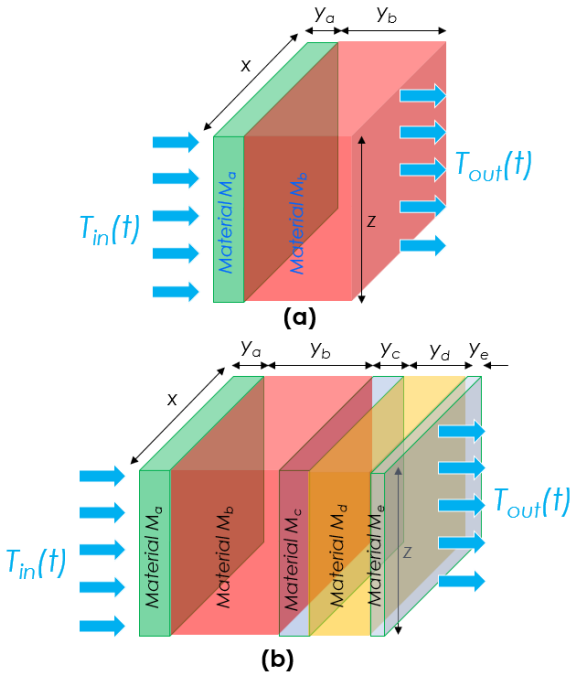

Figure 1: 3D configuration of the piece of wall under study. (a) with 2 layers; (b) with 5 layers.

Similar to the analysis of linear time-invariant (LTI) system, we propose to compute T_{out} analytically with symbolic approach via the thermal transfer function (TTF):

$$TTF(s) = \frac{T_{out}(s)}{T_{in}(s)}, \tag{2}$$

with s is the Laplace variable. To determine this TTF, the modelling method explored in the present paper will be proceeded with the TAN formalism by representing this structure as a Kron's graph topology.

So, in the next section, we will introduce the analytical investigation about the proposed thermal modelling. The thermal structure will be represented in 3D configuration and in its lumped equivalent RC-circuit. Then, the Kron's equivalent graph topology will be defined. The thermal problem metric will be established via branch and mesh space analyses.

3. Analytical description of the TAN formalism based thermal model

3.1. Description of the classical RC-circuit Cauer model

Before the TAN model exploration, let us describe the classical RC model of our structure.

3.1.1. Thermal parameters R and C

Let us denote $\xi = \{a, b, c, d\}$ and the following material layer parameters: λ the thermal conductivity, ρ the material massive density, and δ the specific heat capacity. Based on the thermal circuit theory [4, 17, 22, 35], it is worth to recall

that the ξ^{th}-layer materials can be characterized by the thermal resistances and capacitances :

$$R_{\xi\xi} = \frac{y}{\lambda xz} \tag{3}$$

and

$$C^{\xi\xi} = \frac{yxz}{\lambda}\rho\delta \tag{4}$$

The associated constant time is equal to:

$$\tau(\xi) = R_{\xi\xi}C^{\xi\xi} \tag{5}$$

These parameters which draw the classical equivalent circuit, as described in the next paragraph.

3.1.2. RC equivalent thermal circuit

As reported in [12, 39], the Cauer classical RC lumped circuit of the structure proposed in Fig. 1(a) is shown in Fig. 2. It is composed of respectively by two and five RC-cells in cascade, for 2-layer and 5-layer wall, with input T_{in} and output T_{out}. The reference node presents the environmental temperature T_e. The series branches are with thermal resistance R_ξ and the parallel branches are connected to the reference via capacitance C_ξ. The power corresponding to the thermal fluxes flowing through the branches of the circuit are denoted by P^m with $m = \{1, 2, \ldots, 9, 10\}$.

3.2. TAN modelling based method

The TAN modelling applied to the thermal problem is developed in this paragraph. The method is essentially based on the graph topology, the branch and mesh space analyses and the resolution of the problem metric.

3.2.1. Kron's graph topology

Fig. 3 represents the Kron's equivalent graph of the thermal circuit presented in Fig. 2. The common reference node is still identified with fixed temperature T_e. We can identify in this graph, the thermal circuit source T_{in} and symbolic impedance in function of the Laplace variable s. The analysis of this graph enables to define the number of branches n_b, the number of nodes n_n and the number of meshes n_m. For examples:

- for 2-layer wall, we have $n_b = 4$, $n_n = 2$, and $n_m = 2$.
- for 5-layer wall, $n_b = 10$, $n_n = 5$, and $n_m = 5$.

The parallel impedance are equal to:

$$Z_{\xi\xi} = \frac{1}{sC^{\xi\xi}}, \tag{6}$$

while the impedance of the last branch for two-layer wall is denoted:

$$Zf_2 = R_b + Z_b \tag{7}$$

and for five-layer one is:

$$Zf_5 = R_e + Z_e \tag{8}$$

The TAN in branch and mesh spaces with the descriptions of thermal flux variables will be described in details in the next paragraphs.

3.2.2. TAN equation in the branch space

Based on the TAN formalism [9, 32, 33, 34, 40, 47], the temperature effort and flux, with $\beta = 1, 2, \ldots, n_b$, along the branches are 1-rank tensor. The covariable of the Kron's graph described in Fig. 3 which is represented by the branch temperature source can be written as:

$$T_\beta = \begin{bmatrix} T_{in} & 0 & \ldots & 0 & 0 \end{bmatrix}, \tag{9}$$

and the thermal power flux contravariable can be defined by:

$$P^\beta = \begin{bmatrix} P^1 & P^2 & \ldots & P^9 & P^{10} \end{bmatrix}^T \tag{10}$$

where M^T represents the transpose of the matrix M. The associated thermal branch impedance is a two-rank twice covariable which can be expressed as:

$$Z_{\beta\beta} = \begin{bmatrix} R_a & & & & & & \\ & Z_a & & & 0 & & \\ & & R_b & & & & \\ & & & Z_b & & & \\ & & & & \ddots & & \\ & 0 & & & & R_b & \\ & & & & & & Zf \end{bmatrix} \tag{11}$$

3.2.3. Branch and mesh space connectivity

The main idea behind the connectivity is to solve the problem with a smaller number of variables. For example, instead working in the branch space with β-variable P^β, we can work in the mesh space with μ-variable Q^μ where $\mu = 1, 2, \ldots, n_M$. The link between the branch and mesh spaces can be expressed analytically with the algebraic relation between the branch temperature flux covariable P^β and the mesh temperature flux covariable Q^μ. The connectivity matrix C^μ_β is a 2-rank mixed tensor. It constitutes the bridged between this two 1-rank tensorial object via the Einstein notation:

$$P^\beta = C^\beta_\mu Q^\mu \tag{12}$$

The corresponding matrix relation can be elaborated from the Kron's graph of Fig. 3 and can be summarized by the following equation, respectively for 2-layer and 5-layer wall:

$$\left[C^\mu_\beta\right]_2 = \begin{bmatrix} 1 & 0 \\ 1 & -1 \\ 0 & 1 \end{bmatrix} \tag{13}$$

and

$$\left[C^\mu_\beta\right]_5 = \begin{bmatrix} 1 & 0 & 0 & 0 \\ 1 & -1 & 0 & 0 \\ 0 & 1 & 0 & 0 \\ 0 & 1 & -1 & 0 \\ 0 & 0 & 1 & 0 \\ 0 & 0 & 1 & -1 \\ 0 & 0 & 0 & 1 \end{bmatrix} \tag{14}$$

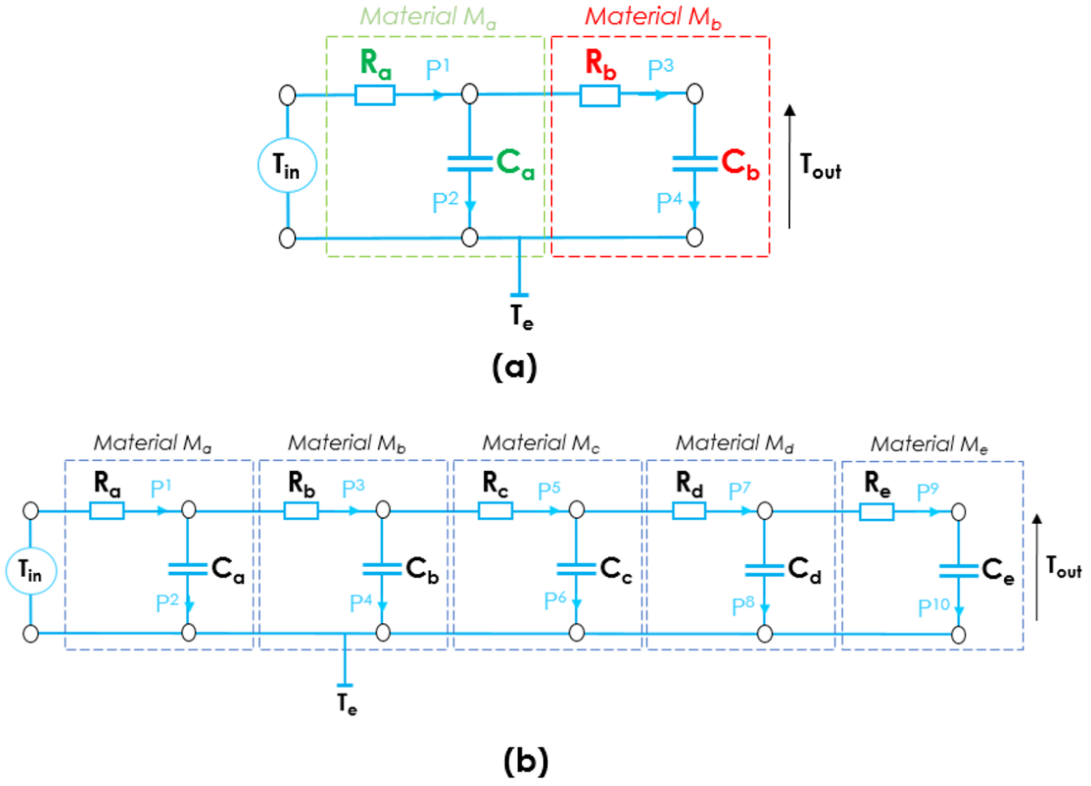

Figure 2: Classical equivalent RC-circuit of the bulk structure: (a) introduced in Fig. 1a; (b) in Fig. 1b

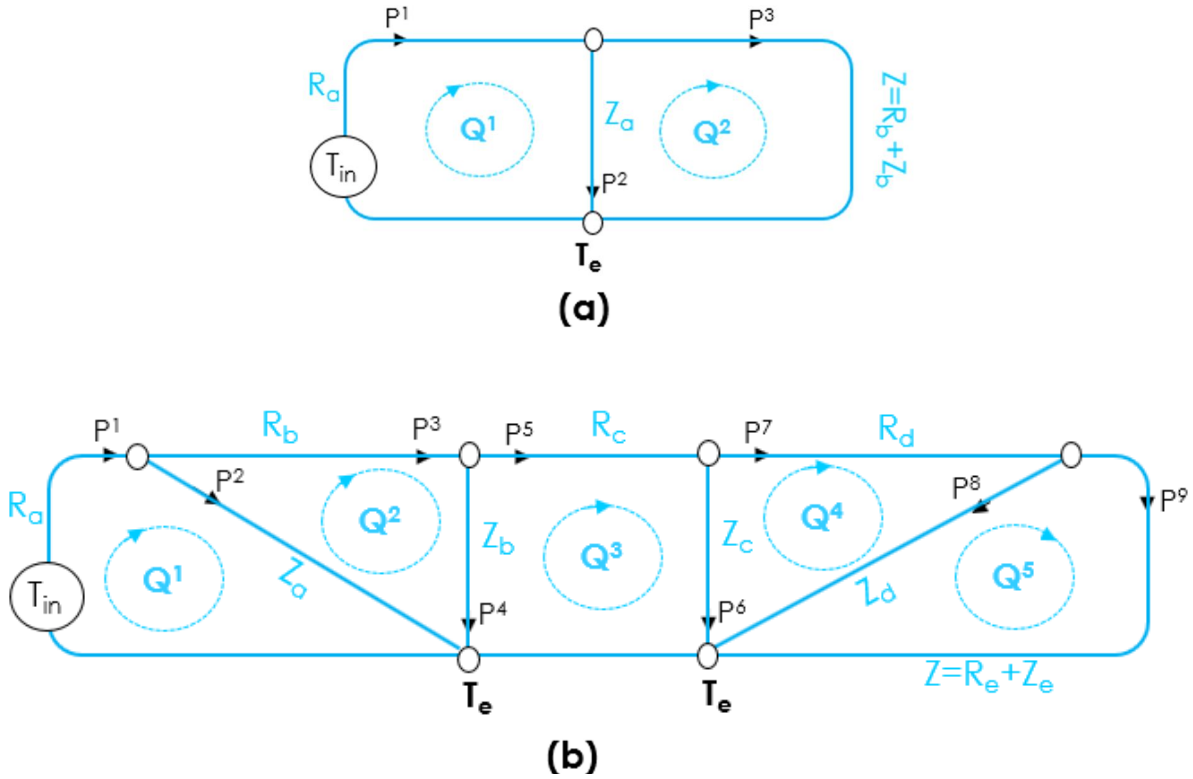

Figure 3: Kron's equivalent graph topology of the structure introduced in: (a) Fig. 1a; (b) Fig. 1b.

3.2.4. TAN equation in the mesh space

In the mesh space, the mesh temperature effort defined in (7) and (8) is transformed as:

$$\left[\Gamma_\mu\right]^T = C_\mu^\beta \left[T_\beta\right]^T \tag{15}$$

where $\left[T^\beta\right]^T$ represents the transpose of $\left[T^\beta\right]$. Similarly, the mesh thermal impedance is defined by:

$$Z_{\mu n} = C_\mu^\beta Z_{\beta\beta} C_n^\beta. \tag{16}$$

Based on the tensor algebra, the indices μ and n are varied from 1 to n_M. Knowing these two parameters, the tensorial equation of our problem can be formulated by the Einstein notation of the generalized Fouriers law (analog to the Ohms law for the electrical circuit):

$$\Gamma_\mu = Z_{\mu n} Q^\mu. \tag{17}$$

This last equation can formulate also the problem metric of the introduced thermal structure in the mesh space. Based on this tensorial formalism, $\left[Z_{\mu n}\right]$ can be assumed as the metric of our thermal network problem. The solution of the problem is given by:

$$q^\mu = Y^{n\mu}\Gamma_\mu \tag{18}$$

with the 2-rank twice contravariable admittance is given by:

$$\left[Y^{n\mu}\right]^T = \left[Z_{\mu n}\right]^{-1}. \tag{19}$$

3.3. Analytical explicited expressions of the piece of wall thermal structure

For sake of a better understanding, we present in this section only the case with 2-layer Wall to concertize the analytical investigation.

So, by applying the previous tensorial relations to our topological graph illustrated in Fig. 3-(top), we have the mesh temperature calculated from (14) is equal to:

$$\Gamma_\mu = \begin{bmatrix} T_{in} & 0 & 0 & 0 \end{bmatrix}. \tag{20}$$

So, the mesh impedance derived from (15) is expressed as:

$$Z_{\mu n} = \begin{bmatrix} R_a + \frac{1}{C_a s} & \frac{-1}{C_a s} \\ \frac{-1}{C_a s} & R_b + \frac{1}{C_a s} + \frac{1}{C_a s} \end{bmatrix} \tag{21}$$

By means of mesh equation (18), we obtain the following mesh thermal flux $[Q^\mu]$ which is constituted by following two components:

$$\begin{bmatrix} Q^1(s) \\ Q^2(s) \end{bmatrix} = \frac{T_{in}(s)}{D_Q(s)} \begin{bmatrix} C_a + C_b + R_b C_a C_b s \\ C_b s \end{bmatrix} \tag{22}$$

with the denominator function is:

$$D_Q(s) = R_a R_b C_a C_b s^2 + \left[R_a(C_a + C_b) + R_b C_b\right] s + 1 \tag{23}$$

Thus, the TTF of the structure introduced in Fig. 1(a) related to materials M_a and M_b are respectively:

$$TTF_a(s) = \frac{R_{bb} C^{bb} s + 1}{\zeta_2 s^2 + \zeta_1 s + 1} \tag{24}$$

$$TTF_b(s) = \frac{1}{\zeta_2 s^2 + \zeta_1 s + 1} \tag{25}$$

where

$$\begin{cases} \zeta_2 = & (R_{aa} C^{aa} R_{bb} C^{bb}) \\ \zeta_1 = & 2R_{aa}(C^{aa} + c_{bb}) + R_{bb} C^{bb}) \end{cases} \tag{26}$$

3.4. Frequency responses

Let us consider f as the frequency variable. By denoting the complex notation angular frequency variable:

$$s = jw = 2\pi f \tag{27}$$

similar to all classical transfer function, the TTF introduced in (24) and (25) can be written in complex form:

$$TTF(jw) = |TTF(jw)| = e^{j\angle TTF(jw)} = TTF(w) e^{j\varphi(w)} \tag{28}$$

The TTF magnitude is given respectively for 2-layer wall and 5-layer one by the following expressions (from (24) and (25)):

$$TTF(w) = |TTF(jw)| = \frac{1}{\sqrt{(1 - \zeta_2 w^2)^2 + \zeta_1^2 w^2}} \tag{29}$$

Similarly, the frequency dependent phase response is expressed as, for each case:

$$\varphi(w) = arctan\left[\frac{w\zeta_1}{1 - \zeta_2 w^2}\right] \tag{30}$$

3.5. Dissipated heat loss estimation

By definition, the instantaneous heat loss is given by:

$$\Delta_T(t) = GV\left[T_{out}(t) - T_{in}(t)\right] \tag{31}$$

where G is the heat losses coefficient. It can take four values according to the characteristics of each layer composing the multilayer wall. As example, for a house that is very well insulated $G = 1$. With little or no insulation, $G = 2$ or $G = 3$, and for a well insulation $G = 1.5$. For the parameter V, it determines the room's volume in $\left[m^3\right]$.

4. Methodology of the thermal problem TAN modelling

The methodology of the developed thermal TAN modelling can be summarized by the following eight steps as described by the following algorithm:

Algorithm 1: Thermal TAN modelling

Begin

Step 1

Definition of the geometrical and physical parameters constituting the thermal structure to be investigated.

Figure 4: Housing in hand to renovate

Step 2
Description of the classical equivalent thermal circuit which can be based on the Cauer RC-model as most of thermal building problem are related to low-order system approach.

Step 3
Drawing the Kron's graph topology equivalent to the thermal circuit described in Step 2.

Step 4
Equating the Kron's graph proposed in Step 3 in the branch space by expressing:
1. The 1-rank tensor covariable representing branch temperature T_β
2. The 1-rank tensor contravariable representing branch thermal flux P_β
3. The 2-rank tensor double covariable representing the branch impedance $Z_{\beta\beta}$

Step 5
Definition of the connectivity expressed in equation (12) which allows to transform the branch space variables into mesh space ones. This quick step is a key point for the TAN formalism because it enables to reduce the number of variable n_b into n_m, knowing that $n_m < n_b$ in any thermal lumped network.

Step 6
Establishing the mesh space variables:
1. The 1-rank tensor covariable representing mesh temperature T_μ
2. The 1-rank tensor contravariable representing branch thermal flux Q^μ
3. The 2-rank tensor double covariable representing the mesh impedance $Z_{\mu n}$

Step 7
Solving the problem with the preliminary solution represented by Q_n.

Step 8
Determination of the temperature of each element constituting the wall to be investigated and also calculation of further parameters as the losses.

5. Results and discussion

5.1. Description of the piece-of-wall proof-of-concept

To concretize the previous analytical investigation, the present section introduces the validation results with a study case example. We apply the methodology to accompany the retrofitting of an old residential housing located in the north of the France (Fig. 4). The house is located precisely in Rinxent, it was built from 1848 and its surface is $60m^2$. Today, the walls are composed of two layers of which one by stones of thickness of $50cm$ and the other by a coating of $5cm$. The owners would like to isolate their residence by hemp-lime plaster for the walls. But they would like to know the efficiency of this insulation compared with another matter one before starting work.

For that end, three scenarios are studied in this paper. For each of them, we consider distinct insulation material M_{Ci} with $i = \{1, 2, 3\}$ combined with other layers as illustrated in Table 1. Then, time-domain results will be discussed by considering an arbitrary variation of temperature which propagates through the wall; in other words during this study we consider a free-heating (and also cooling) device case. Thereafter, to verify the effectiveness of the TAN modelling, frequency analyses will be examined by comparing the computed TTF from TAN formalism and simulation.
As previously said, to realize the thermal modelling, we have the associated physical and geometrical parameters indicated in Table 1. Based on these parameters, the lumped thermal circuit resistances and capacitances are given in Table 2.

5.2. Walls performance analysis by thermal excitation

The dynamic responses of building system are usually analyzed in the time-domain [4, 14, 22, 35]. The TAN model enables to compute also the transient responses of any thermal structure. In the present study, we illustrate the feasibility of this time domain analysis with two application cases based on unit step and arbitrary time dependent input temperature responses.

So, this study is necessary because it allows the understanding of the time response of each insulation material. In other words, we can observe the influence of the input temperature at the output temperature and the speed at which this exchange

Table 1: Parameters of the considered materials: Rinxent housing

Test	Layer	Materials	Thickness $y\,[m]$	Thermal resistance $R\left[m^2K/W\right]$	Thermal conductivity $\lambda\,[W/mK]$	Thermal capacity $C\left[W/m^2K\right]$
(a)	M_A	Stones	0.50	0.14	3.5	7.14
	M_B	Lime and sands	0.06	0.55	0.110	1.82
	M_{C1}	Hemp-lime	0.15	0.75	0.2	1.33
	M_D	Marfolding coating	0.05	0.06	0.83	16.66
	M_E	Finishing plaster	0.05	0.45	0.110	2.22
(b)	M_A	Stones	0.50	0.14	3.5	7.14
	M_B	Lime and sands	0.06	0.55	0.110	1.82
	M_{C2}	Cellulose wadding	0.20	5.26	0.038	0.19
	M_D	Marfolding coating	0.05	0.06	0.83	16.66
	M_E	Finishing plaster	0.05	0.45	0.110	2.22
(c)	M_A	Stones	0.50	0.14	3.5	7.14
	M_B	Lime and sands	0.06	0.55	0.110	1.82
	M_{C3}	Expanded polystyrene	0.16	5	0.032	0.24
	M_D	Marfolding coating	0.05	0.06	0.83	16.66
	M_E	Finishing plaster	0.05	0.45	0.110	2.22

Table 2: Parameters of the considered materials: Rinxent housing

Test	Layer	Lumped element	Value [ms]
(a)	M_A	τ_a	99.96
	M_B	τ_b	100.1
	M_{C1}	τ_{c1}	98.75
	M_D	τ_d	100
	M_E	τ_e	99.9
(b)	M_A	τ_a	99.96
	M_B	τ_b	100.1
	M_{C2}	τ_{c2}	105.2
	M_D	τ_d	100
	M_E	τ_e	99.9
(c)	M_A	τ_a	99.96
	M_B	τ_b	100.1
	M_{C3}	τ_{c3}	120
	M_D	τ_d	100
	M_E	τ_e	99.9

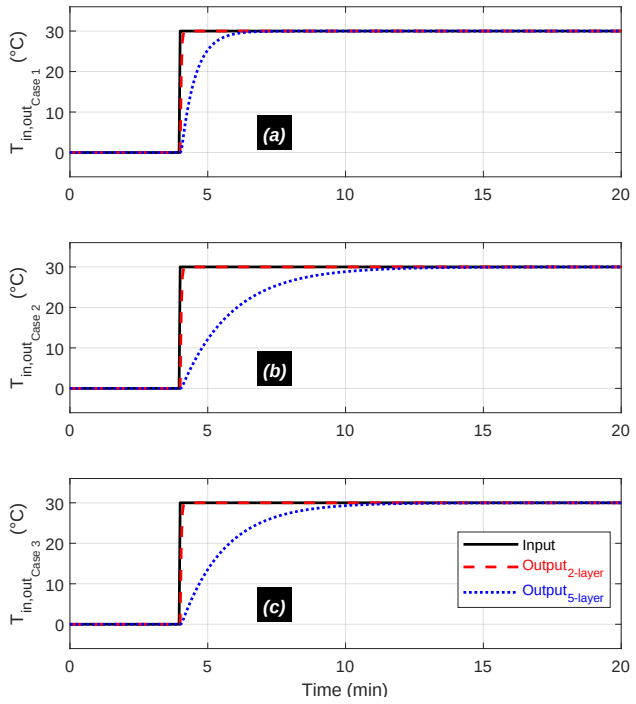

Figure 5: Unit step response with amplitude $T_{max} = 30^oC$ from the 5-layer wall TAN model

takes place. Fig. 5 (red dashed line) shows us for instance for the 2-layer walls that barely after $10s$ the input and output temperatures are identical. That means the current building with 2-layer walls has no thermal comfort neither in summer nor in winter seasons.Whereas for the structure with 5-layer wall, the exchange is done only after about $12mn$ which defines the thermal inertia of the building (Fig. 5: blue dashed line). In other terms, for a free-heating system configuration, and by observing an arbitrary input temperature (Fig. 6-left), the thermal transfer is delayed by this time thermal inertia, and also determine prior the temperature comfort in the housing.

Moreover, reader can see that the experiment is done during only $20mn$, time required to the output temperature to meet the final value of the input one. Thus, we can also say that this method can be used for the fast prediction of the time-dependent dynamics of the heat flow through the building.

5.3. Walls passivity analysis by thermal frequency response

For the wider insight about the TTF behavior, frequency responses of each case were analysed were in the frequency range from $0Hz$ to $1Hz$. Comparisons between the frequency responses from TAN computed with Matlab and commercial tool simulations were performed. The obtained result from the TTF magnitude expressed in (29) is displayed in Fig. 7. Furthermore, the Matlab TAN computations with the phase response expressed in (30) give the results presented in Fig. 8. As expected, the 5-layer wall behaves as a classical passive system. The system presents a typical high-order passive filter behavior.

Therefore, these results show us that depending the insulation material that will be chosen to renovate the building (case (a-b-c)), the output temperature can't change before $t = 10s$. In other terms if the input temperature observed a quick variation before this time horizon, it can't influence the thermal behavior of the building. This is confirmed by Fig. 8 where the phase response increased when the input temperature observed a quick variation.

The choice of type of insulation plays an important role then in the building renovation strategy. In fact, by combining results in Fig. 6 and 8 slot $[0-5mn]$, it can be seen that the outside temperature only changes after $2mn$. Also for the slot $[10-15mn]$, we can observe the performance of the insulation material by comparing the input-output temperature behavior during this period. The internal temperature of the housing is globally stable, expect for the case (a).

5.4. Estimation of the wall energy losses

Based on the previous results with the arbitrary waveform input temperature, the dissipated heat loss from the wall were calculated and realized according to the parameter value reported into Table 3.

Fig. 6-right side displays the instantaneous heat loss dynamic for the each configuration and Table 4 below summarizes the average heat loss results obtained. So, the choice of insulation can be sen as a compromise between its performance and its price. For this experiment, we can suggest the insulation used in the case (b) to renovate the housing under the investigation.

6. Conclusions and further work

An innovative method of building wall thermal modelling is developed in this paper. The thermal dynamic model is based on the Kron's method. This unfamiliar computation approach is originally implemented with the Tensorial Analysis of Networks (TAN) formalism. The feasibility of the model is studied with challenging application examples of a two and five-layer piece of wall. For each example case, an analytical

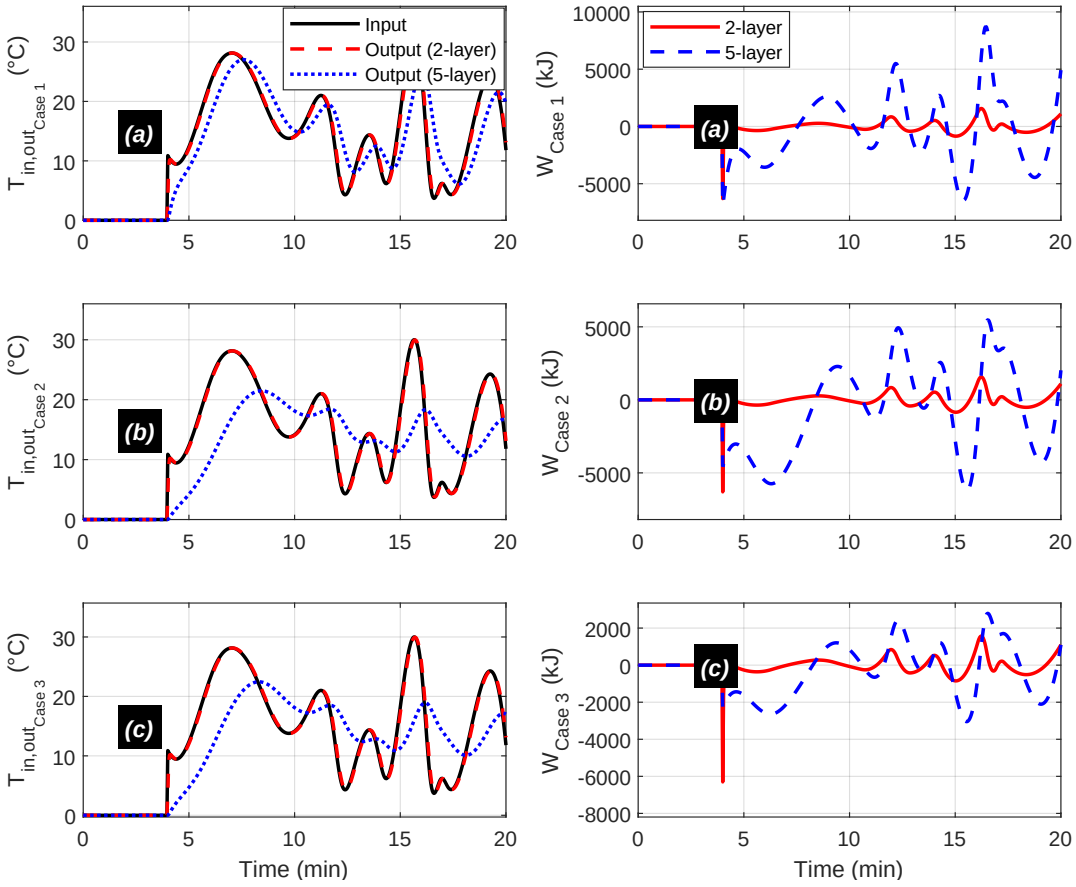

Figure 6: (left) Transient responses with arbitrary input temperature and (right) Instantaneous heat lost from the 5-layer wall TAN model

Table 3: Thermal dissipation loss parameters.

Layer number	Volume $[m^3]$	Total thickness $[m]$	Total thermal conductivity $[W/mK]$	Thermal loss coefficient G	Remark
2	210	0.56	3.61	3	
5	210	0.81	4.75	1.5	Case (a)
5	210	0.86	4.59	1	Case (b)
5	210	0.82	4.58	1.5	Case (c)

Table 4: Average thermal dissipated losses per case

	5-layer			2-layer
	Case (a)	Case (b)	Case (c)	
Heat-losses $[KWh]$	16.53	11.13	10.29	27.23

methodology of the thermal TAN modelling is described with the following original aspects:

- the effectiveness of the TAN model for solving the building wall computation problems,
- in difference to classical thermal modelling methods, realistic cases of 3-D problem are considered under physical and geometrical material parameters. The treated proof-of-concept structures are from a residential building located in the north of the France, subject to a retrofit problem.

Moreover, the TAN modelling presents a significant advantage as:

- a fast computation time in both time- and frequency-domain,
- a good accuracy to predict the walls performance according to an arbitrary thermal excitation,
- a possibility of geometrical location of the heat flow through the building is given,

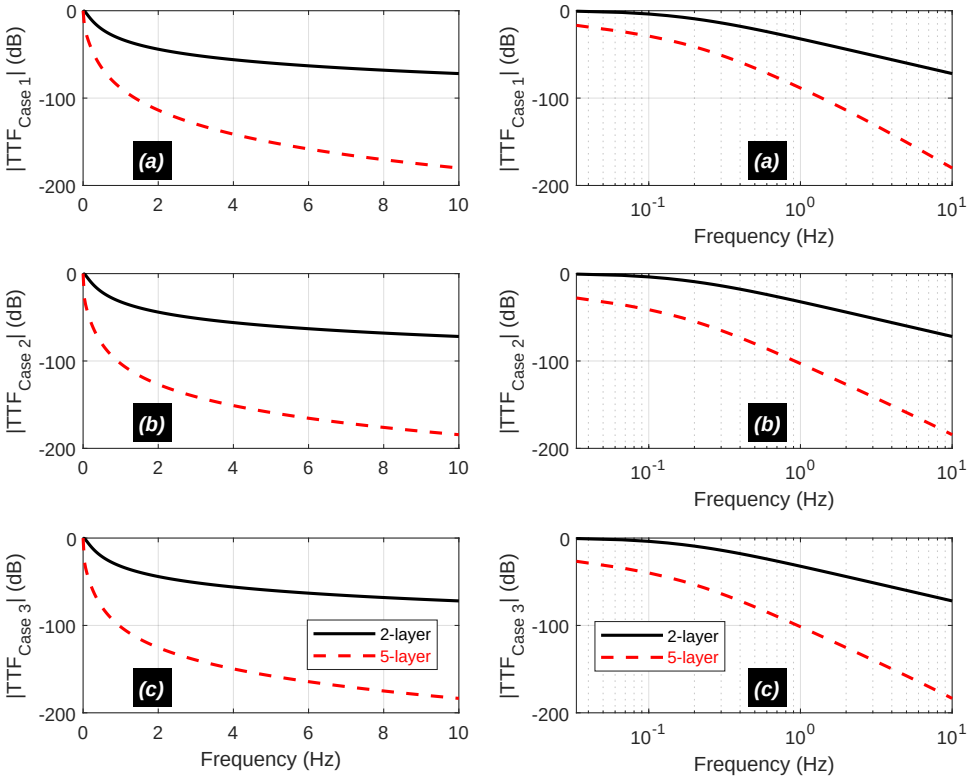

Figure 7: TTF magnitude per test cases in (left) linear and (right) semi-log plots

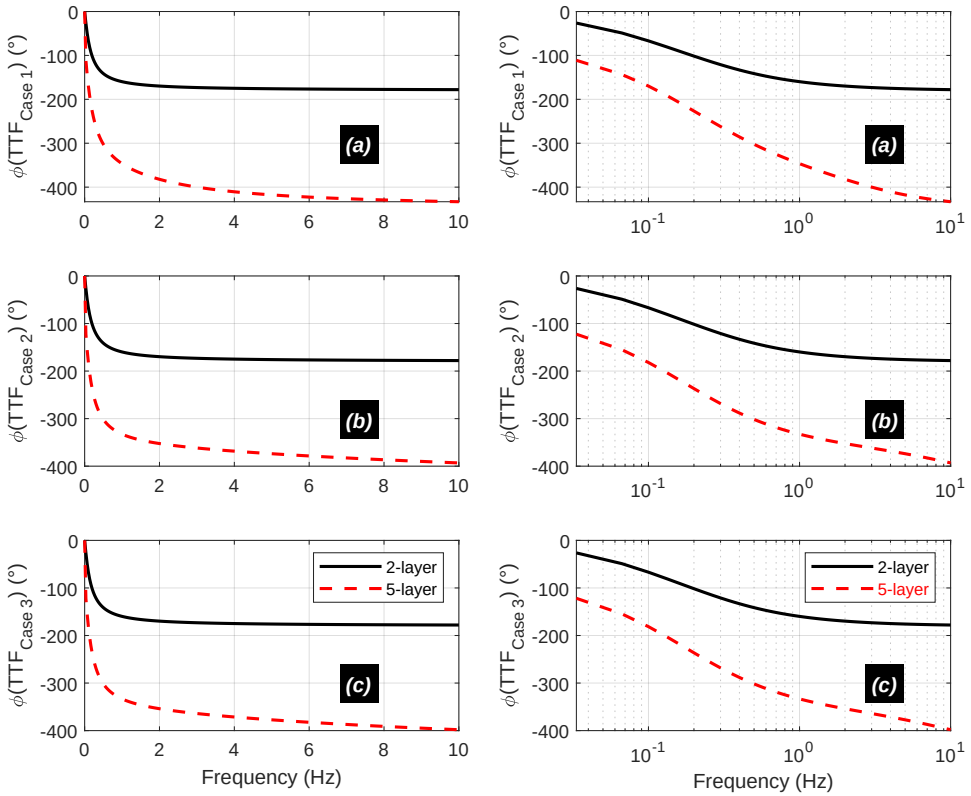

Figure 8: TTF phase response per test cases in (left) linear and (right) semi-log plots

- the possibility to estimate the thermal loss for different parameters of the material constituting the piece of wall,
- and finally the model allows to provide some recommendations to perform the building retrofit strategies.

In the future, the application of the TAN model for solving thermal loss problems of residential building composed by several rooms and even several floors, by considering the geometrical sizes, will be the logical continuation of this work. Moreover, this model can be exploited with its major competitive advantage. For instance for future researches on Multiphysics engineering problems, for computing simultaneously both thermal and electrical circuit problems in the smart building, and modelling of higher level of engineering systems including automation subsystem for controlling electrical circuits.

Acknowledgements

This research work was supported by the European project "SHINE: Sustainable Houses in Inclusive Neighbourhoods". A project granted by Interreg 2 Seas and the European Regional Development Fund.

References

[1] A. Al-janabi, M. Kavgic, A. Mohammadzadeh, and A. Azzouz. Comparison of energyplus and ies to model a complex university buildingusing three scenarios: Free-floating, ideal air load system, and detailed. *Journal of Building Engineering*, 22:262–280, 2019.

[2] S. Al-Sanea and M. Zedan. Improving thermal performance of building walls by optimizing insulation layer distribution and thickness for same thermal mass. *Appl Energy*, 88:3113–3124, 2011.

[3] F. Almeida, D. Zhang, A. Fung, and W. Leong. Investigation of multilayered phase-change-material modeling in esp-r. In *Proc. International high Performance Buildings Conference*, 2010.

[4] K. Andersen, H. Madsen, and L. Hansen. Modelling the heat dynamic of a building using stochastic differential equations. *Energy and Buildings*, 31:13–24, 2000.

[5] M. Benzaama, S. Menhoudj, K. Kontoleon, A. Mokhtari, and M. Lekhal. Investigation of the thermal behavior of a combined geothermal system for cooling with regards to algeria's climate. *Sustainable Cities and Society*, 43:121–133, 2018.

[6] M. Benzaama, L. Rajaoarisoa, B. Ajib, and S. Lecoeuche. Data-driven approach for modelling the thermal dynamics of residential buildings using a piecewise ARX model. In *Proc. 16th International Building Simulation Conference and Exhibition*, September 2019.

[7] D. Bond, W. Clark, and M. Kimber. Configuring wall layers for improved insulation performance. *Appl Energy*, 112:235–245, 2013.

[8] D. Cao, T. Q. Bui, and A.-L. Kj⊘niksen. Thermal analysis of multilayer walls containing geopolymer concrete and phase change materials for building applications. *Energy*, 186:115792, 2019.

[9] C. Cholachue, B. Ravelo, A. Simoens, and A. Fathallah. Fast s-parameter tan model of n-port lumped structures. *IEEE Access*, 7(1):72505–72517, 2019.

[10] J. Clarke. Energy Simulation in Building Design. Technical report, Oxford, 2001.

[11] D. Crawley, J. Hand, K. M., and G. B.T. Contrasting the capabilities of building energy performance simulation programs. *Building and Environment*, 43(4):661–673, 2008.

[12] J. N. Davidson, D. A. Stone, and M. P. Foster. Required cauer network order for modelling of thermal transfer impedance. *Electronics Letters*, 50(4):260–262, 2014.

[13] K. Deng, P. Barooah, G. Mehta, and S. Meyn. Building thermal model reduction via aggregation of states. *American Control Conference (ACC)*, 28:5118–5123, 2010.

[14] F. Déqué, F. Ollivier, and A. Poblador. Grey boxes used to represent buildings with a minimum number of geometric and thermal parameters. *Energy and Buildings*, 31:29–35, 2000.

[15] U. Directive UE. Directive relative à l'efficacité énergétique, modifiant les directives 2009/125/ce et 2010/30/ue. *J.O. de l'Union européenne*, 14/11, 2012.

[16] J. Dobbs and B. Hencey. Automatic model reduction in architecture: A window into building thermal structure. In *Proc. 5th National Conference of IBPSA-USA. Madison, Wisconsin*, August 2012.

[17] G. Fraisse, C. Viardot, O. Lafabrie, and G. Achard. Development of a simplified and accurate building model based on electrical analogy. *Energy and Buildings*, 34:1017–1031, 2002.

[18] S. Ginestet, T. Bouache, K. Limam, and G. Lindner. Thermal identification of building multilayer walls using reflective newton alogrithm applied to quadrupole modelling. *Energy and Buildings*, 60:139–145, 2013.

[19] P. Gori, C. Guattari, L. Evangelisti, and F. Asdrubali. Design criteria for improving insulation effectiveness of multilayer walls. *Int J Heat Mass Transf*, 103:349–359, 2016.

[20] D. S. Gouda, M. and C. Underwood. Low-order model for the simulation of a building and its heating system. *Building Services Energy Research Technology*, 21(3):199–208, 2000.

[21] D. S. Gouda, M. and C. Underwood. Building thermal model reduction using nonlinear constrained optimization. *Building and environment*, 37:1255–1265, 2002.

[22] M. Gough. *Modelling heat flow in buildings: an eigenfunction approach*. PhD thesis, University of Cambridge, 1982.

[23] S. Goyal and P. Barooah. A method for model-reduction of nonlinear thermal dynamics of multi-zone buildings. *Energy and Buildings*, 47:332–340, 2012.

[24] D. Han and J. Lim. Smart home energy management system using ieee 802.15.4 and zigbee. *Consumer Electronics, IEEE Transactions*, pages 1403–1410, 2010.

[25] G. Kron. *Tensor Analysis of Networks*. Wiley, New York, Chapman and Hall, London, 1939.

[26] P. Lagonote, E. Bertin, and J.-B. Saulnier. Analyse de la qualité de modèles nodaux réduits à l'aide de la méthode des quadripoles (in french). *International Journal Thermal Sciences Elsevier*, 38:51–65, 1999.

[27] J. Lefebre, B. J., and N. A. Simulation of the thermal behaviour of a room by reduced order numerical methods. *Revue Génerale de Thermique*, 3426:106–114, 1987.

[28] K. Liu, T.-Z. Liu, P. Jian, and Y. Lin. The re-optimization strategy of multi-layer hybrid building's cooling and heating load soft sensing technology research based on temperature interval and hierarchical modeling techniques. *Sustainable Cities and Society*, 38:42–54, 2018.

[29] H. Madsen and J. Holst. Estimation of continuous time models for the heat dynamics of a building. *Energy and Buildings*, 22:67–79, 1995.

[30] J. Massana, C. Pous, L. Burgas, J. Melendez, and J. Colomer. Identifying services for short-term load forecasting using data driven models in a smart city platform. *Sustainable Cities and Society*, 28:108–117, 2017.

[31] E. Mathews, P. Richards, and C. Lombard. A first-order thermal model for building design. *Energy and Buildings*, 21:133–145, 1994.

[32] O. Maurice. *Elements of theory for electromagnetic compatibility and systems*. Bookelis, Aix en Provence, France, 2017.

[33] O. Maurice. Proposal of a method for systematic electrothermal analysis. HAL-02054761, Feb. 2019.

[34] O. Maurice, A. Reineix, P. Durand, and F. Dubois. Kron's method and cell complexes for magnetomotive and electromotive forces. *Int. J. Applied Mathematics*, 44(4):183–191, 2014.

[35] N. Milbank and J. Holst. Thermal response and the admittance procedure. *Building Services Engineering*, 42:67–79, 1995.

[36] R. Missaoui, H. Joumaa, S. Ploix, and S. Bacha. Managing energy smart homes according to energy prices: Analysis of a building energy management system. *Energy and Buildings*, 71:155–167, 2014.

[37] M. Ozel and K. Pihtili. Optimum location and distribution of insulation layers on building walls with various orientations. *Build Environ*,

42:3051–3059, 2007.

[38] B. Ravelo. Multiphysics model of microstrip structure under high voltage pulse excitation. *IEEE Journal on Multiscale and Multiphysics Computational Techniques (JMMCT)*, 3(1):88–96, 2018.

[39] B. Ravelo, B. Agnus, and T. Carras S.and Davin. Cauer ladder inspired kron-branin modelling of thermal 1d diffusion. *IEEE Trans. Circuits and Systems II: Express Briefs, Early Access*, 3:1–5, 2019.

[40] B. Ravelo and O. Maurice. Kron-braning modeling of y-y-tree interconnects for the pcb signal integrity analysis. *IEEE Trans. Electromagnetic Compatibility*, 59(2):411–419, 2017.

[41] K. Rick, v. S. Jos, and S. Henk. Inverse modeling of simplified hygrothermal building models to predict and characterize indoor climates. *Building and Environment*, 68:87–99, 2013.

[42] S. Royer, S. Thil, T. Talbert, and M. Polit. A procedure for modeling buildings and their thermal zones usingco-simulation and system identification. *Energy and Buildings*, 78:231–237, 2014.

[43] J. Siroky, F. Oldewurtel, J. Cigler, and S. Prvara. Experimental analysis of model predictive control for an energy efficient building heating system. *Applied Energy*, 88:3079–3087, 2011.

[44] R. Sonderegger. Harmonic analysis of building thermal response applied to the optimal location of insulation within the walls. *Energy and Buildings*, 1977(1):131–140, 2008.

[45] A. Thavlov and H. Bindner. Thermal models for intelligent heating of buildings. *In Proceedings of the Int. Conference on Applied Energy, ICAE 2012*, July 5-8:A10591–A106000, 2012.

[46] S. Wang and X. Xu. Simplified building model for transient thermal performance estimation using ga-based parameter identification. *International Journal of Thermal Sciences*, 45:419–432, 2006.

[47] Z. Xu, B. Ravelo, S. Lalléchère, O. Maurice, and F. Wan. Kron-branin modeling of symmetric star tree interconnect. *Int. J. Circ. Theor. Appl.*, 47(3):391–405, 2019.